

## The structural transformation from metallic glass to nanostructure and improvement of the magnetic properties by using pulse annealing method (PAM)

R. ŞAHİNGÖZ<sup>a\*</sup>, M. EROL<sup>a</sup>, S. YILMAZ<sup>a</sup>, S. KAZAN<sup>b</sup>

<sup>a</sup>Bozok University, Department of Physics, 66200, Yozgat, Turkey

<sup>b</sup>Gebze Institute of Technology, Department of Physics, 41400, Gebze, Kocaeli, Turkey

\*Corresponding Author: [sahingoz@erciyes.edu.tr](mailto:sahingoz@erciyes.edu.tr)

### Abstract

Improvement of the magnetic properties and structural transformation of metallic glasses can be done by using Pulse Annealing Method (PAM). The basic problems of the conventional annealing treatments are oxidation and difficulties about managing the crystallization steps. PAM overcomes these limitations and cause low coercivity in contrast to high susceptibility in milliseconds. Recent works investigated that partially nucleation, partially crystallization and nanostructure of the materials are preferable from the industrial application point of view and it is easy to approach to these advantageous by PAM. In this study, PAM was explained and schematic illustration was given. Metallic glasses  $\text{Fe}_{40}\text{Ni}_{40}\text{B}_{20}$ ,  $\text{Fe}_{39}\text{Ni}_{39}\text{Mo}_4\text{Si}_6\text{B}_{12}$  and  $\text{Fe}_{77}\text{Cr}_2\text{Si}_5\text{B}_{16}$  were annealed by PAM. Coercivity ( $H_c$ ) and susceptibility ( $\chi$ ) values were measured after some steps of electrical pulse application to the samples.  $H_c$ -Pulse numbers and  $\chi$ -Pulse numbers plots of the samples were given. It has to be pointed out that the structures of the samples are transformed from metallic glass to nanostructure with PAM in milliseconds. Ferromagnetic resonance (FMR) studies supporting the occurrence of nanostructure by PAM treatments were also given. FMR studies of the samples show the magnetic anisotropy and improvement of it by PAM were also given.

(Received February 4, 2009; accepted March 02, 2009)

**Keywords:** Coercivity, magnetic susceptibility, metallic glass, pulse annealing, nanostructure, FMR, magnetic anisotropy.

### 1. Introduction

The field of nanostructured materials has rapidly grown in the last decades. One of the key issues for the researchers is controlling the structures of materials on the nanometric scale. Almost twenty years ago it is found that by decreasing the average crystal size of a material to nanometric scale, the magnetic losses in some materials can be reduced. The improvement magnetic properties and structural transformation for metallic glasses and amorphous ribbons can be done by thermal treatments such as flash annealing [1-2] and current annealing methods where a DC current was applied for a short time [3-6].

Samples were produced by planar flow casting method. Melt spinning method (and planar flow casting method) have some advantages. Because it requires a small quantity of materials, it is fast and reliable process, with reduced costs compared other techniques, and gives completely reproducible results. Also it is very useful because the amorphous structure of the as-obtained ribbons can be easily transformed into nano-sized crystalline grains by subsequent heat treatments [7].

In this study, metallic glasses were heat treated by using Pulse Annealing Method (PAM). The details of PAM are explained in Ref. [8]. High speed crystallization succeeded by using PAM which caused reduction in the grain size, improvement of the homogeneity and increase in the coercivity of the sample [9]. In this study we achieved that metallic glasses or rapidly solidified amorphous alloys can be made nanostructure and reduced oxidation by PAM treatment. The profile of PAM treatment can be seen also from the FMR studies, that this method provides us many advantageous such as short annealing time without oxidation etc.

## 2. Experimental Procedure

### 2.1. Sample Preparation

Rapidly quenched metallic glasses  $\text{Fe}_{40}\text{Ni}_{40}\text{B}_{20}$ ,  $\text{Fe}_{39}\text{Ni}_{39}\text{Mo}_4\text{Si}_6\text{B}_{12}$  and  $\text{Fe}_{77}\text{Cr}_2\text{Si}_5\text{B}_{16}$  were prepared by planar-flow casting method. Specimens were prepared from reels to relevant dimensions of  $50.0 \times 2.5 \times 0.030$  mm,  $50.0 \times 2.5 \times 0.025$  mm and  $50.0 \times 2.5 \times 0.022$  mm, respectively. Samples were cleaned carefully by acetone and dried in the desiccator for protecting from oxidation. Specimens were taken from the best part of the ribbons (smooth, clean and notch less parts). Dirtiness on the specimens can cause corrosion in the presence of the grease, during heat treatment. XRD analyses of the samples were taken by BRUKER AXS D8 advance model and SEM analyses were taken by computer controlled LEO 440 digital system.

### 2.2. Annealing of the Samples

High current flowing through the samples causes to high annealing in a very short time (in millisecond) by PAM. PAM is a preferable method to the other classical annealing methods because of its outstanding properties such as reproducibility and annealing without oxidation. It is also very quick and controllable treatment in order to obtain desirable structure of the samples. It is easy to provide optimum annealing conditions in this method. Crucial point of this method is to control of the grain size and nanocrystallization of the samples. This method also requires no inert atmosphere, because there is no enough time for oxidation. Annealing can be performed in air. It is known that higher temperatures caused to lower grain sizes compared to conventional treatments. The schematic representation of the PAM diagram is given in Fig. 1. It can be seen from the block diagram of the pulse annealing test circuit that heating of the samples by constant high current in a short duration of time is the main goal of the method.

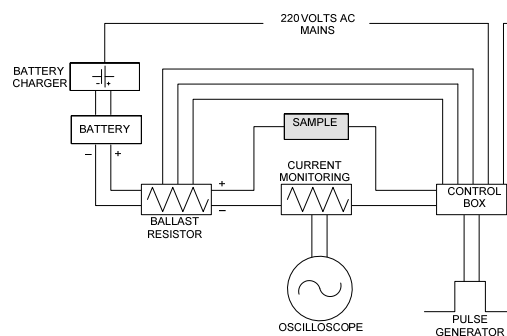


Fig. 1. The schematic representation of Pulse Annealing Method (PAM).

We used a car battery as a constant voltage source in order to get exactly constant current. 10.87 Volts – 20 Amperes constant current can be available from the circuit shown in Fig. 1 during each steps of pulse heating process. The metallic glass target was heated by absolutely constant current in a very short time without oxidation. The optimum pulse width can be obtained and controlled by pulse generator. The pulse width were depending on the resistance of the samples, however, width was fixed at 50 or 55 milliseconds.

### 2.3. Magnetic Coercivity and Susceptibility Studies

The metallic glasses  $\text{Fe}_{40}\text{Ni}_{40}\text{B}_{20}$ ,  $\text{Fe}_{39}\text{Ni}_{139}\text{Mo}_4\text{Si}_6\text{B}_{12}$  and  $\text{Fe}_{77}\text{Cr}_2\text{Si}_5\text{B}_{16}$  were multiple annealed by pulse where the electrical resistances of the samples were between 0.5-0.7 Ohms. The coercivity ( $H_c$ ) values of as-received samples were measured by using a DC major hysteresis loop measurement system [10]. Susceptibility ( $\chi$ ) values were calculated by using the data obtained from hysteresis loops. The coercivity and susceptibility measurements were plotted against pulse numbers. Stress relief of the samples can be followed by the first step of the M-H loops and Susceptibility - Pulse Number graphs.

### 2.4. FMR Studies

The ferromagnetic resonance (FMR) technique have been used to determine the magnetic anisotropies of as-quenched and annealed  $\text{Fe}_{40}\text{Ni}_{40}\text{B}_{20}$  bulk sample by PAM. The FMR measurements were carried out using commercial EMX X-Band (9.8 GHz) spectrometer equipped with pole-cap which provides a DC magnetic field up to the 22 kG. A gonio-meter was used to rotate the sample holder which is parallel to the microwave magnetic field and perpendicular to the applied static magnetic field. The sample was replaced to sample holder in two different geometries. For the in-plane geometry the sample was attached horizontally to the bottom edge of sample holder. During rotations the normal of film plane remained parallel to the microwave magnetic field, but external DC magnetic field was aligned at different orientation with respect to the sample axis. At out-of-plane geometry, the sample was attached to the flat platform of sample holder where the magnetic field of microwave lie in film plane during measurement and static magnetic field is rotated from the sample plane to surface normal. The used coordinate axes and relative orientation of applied static magnetic field and magnetization vector were illustrated in Fig. 2. The field derivative of microwave power absorption ( $dP/dH$ ) was recorded as a function of the DC field. To obtain intensities of FMR signals, the double digital integration of the resonance curves were performed using Bruker WINEPR software package.

The FMR spectra were analyzed by the fallowing model. The free energy for the magnetization

$$\begin{aligned} E &= E_z + E_b \\ E_z &= -M_0 H (\sin \theta \sin \theta_H \cos(\phi_H - \phi) + \cos \theta \cos \theta_H) \\ E_b &= K_{eff} \cos^2 \theta, \quad K_{eff} = (2\pi M_0 - K_{\perp}) \end{aligned} \quad (1)$$

where  $E_z$  and  $E_b$  are r the Zeeman and the bulk (overall) anisotropy energy terms, respectively.  $M_0$  is the saturation magnetization,  $\theta$  and  $\phi$  are the spherical angles for the  $M$ ,  $\theta_H$  is the usual spherical polar angle for the applied field  $H$  as shown in Fig. 2.  $K_{eff}$  is the effective bulk (shape-demagnetizing) anisotropy constant.

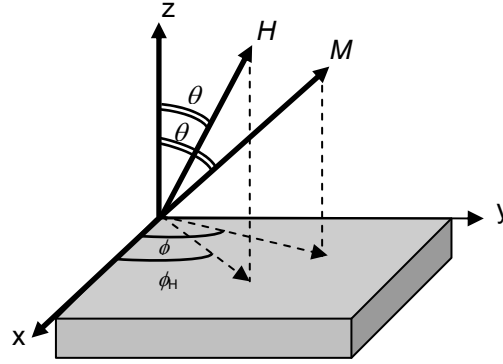


Fig. 2. Coordinate system and relative orientation of the sample with respect to the applied static magnetic field ( $H$ ) and static magnetization ( $M$ ).

For the resonance condition, we used the classical resonance equation given in many ferromagnetic resonance studies in literature:

$$\frac{\omega_o}{\gamma} = \frac{1}{M \sin \theta} (E_{\theta\theta} E_{\varphi\varphi} - E_{\theta\varphi}^2)^{1/2} \quad (2)$$

By using the Eq. (2), we get the following resonance equation:

$$\left( \frac{\omega}{\gamma} \right)^2 = \frac{[H \cos(\theta_H - \theta) - 4\pi M_{eff} \cos^2 \theta]}{[H \cos(\theta_H - \theta) - 4\pi M_{eff} \cos 2\theta]} \quad (3)$$

### 3. Results and Discussions

#### 3.1. Coercivity ( $H_c$ ) and Susceptibility ( $\chi$ )

##### Results

At higher current levels, i.e., in pulse-annealed samples, the magnetic coercivity was minimized rapidly as shown in Fig. 3, Fig. 4 and Fig. 5. Time to reach  $H_{c(\min)}$  with pulse annealing were in milliseconds range which was not possible in the previous works [7, 11].

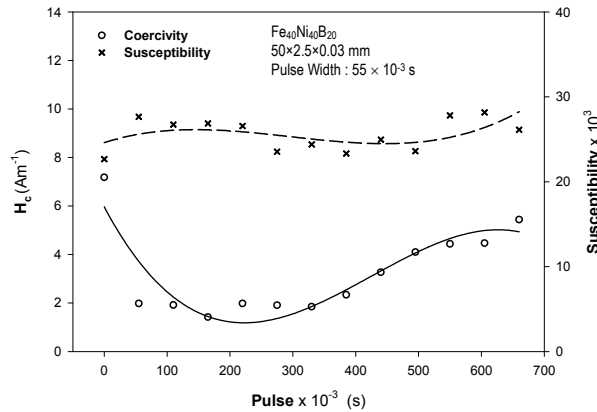


Fig 3.  $H_c$  and  $\chi$  as a function of Pulse Number for  $Fe_{40}Ni_{40}B_{20}$  metallic glass.

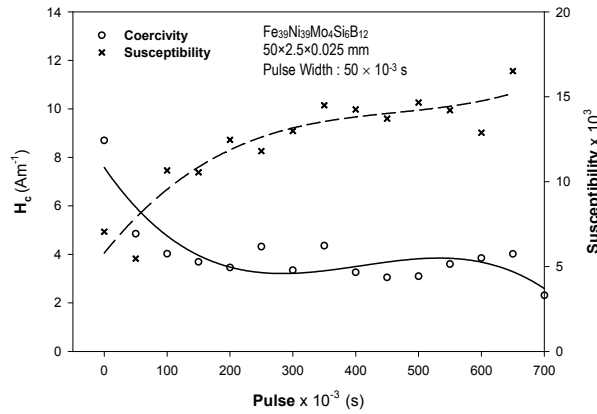


Fig 4.  $H_c$  and  $\chi$  as a function of Pulse Number for  $Fe_{39}Ni_{39}Mo_4Si_6B_{12}$  metallic glass.

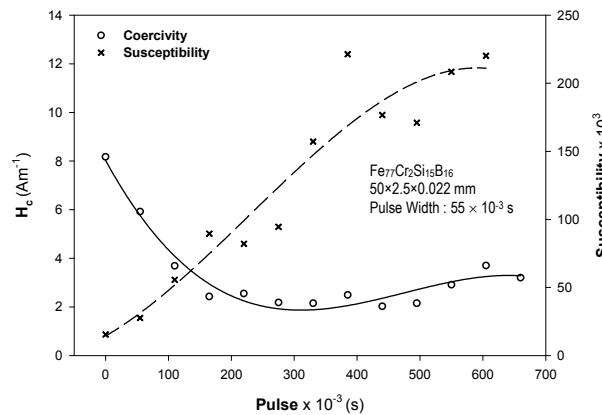


Fig 5.  $H_c$  and  $\chi$  as a function of Pulse Number for  $Fe_{77}Cr_2Si_5B_{16}$  metallic glass.

As it can be seen from Fig. 3, after 165 ms annealing period (in 3 steps) of  $Fe_{40}Ni_{40}B_{20}$ ; the coercivity approached to a minimum value of 1.70 A/m. There was no evidence of crystallization observed, but, stress relaxation almost finished. Susceptibility of the  $Fe_{40}Ni_{40}B_{20}$  was given at the same Fig. 3 as well.  $\chi$  starts roughly from  $20 \times 10^3$  and reaches to maximum  $30 \times 10^3$ . So this is expected because of the magnetization of the samples related to preparation processes, composition, shape etc. It can be seen from Fig. 3 that nucleation and starting of nanocrystallisation caused to increase of  $H_c$  and  $\chi$  as well. Joule heating means high temperature in a short time. In this case even in air condition, there was not much time for oxidation. This is one of the main reason for high coercivity.

As-received  $Fe_{39}Ni_{39}Mo_4Si_6B_{12}$  was prepared at  $50 \times 2.5 \times 0.025$  mm dimensions and  $H_c$  and  $\chi$  were plotted as a function of Pulse Numbers as shown in Fig. 4. As it is known that while  $H_c$  decreases  $\chi$  increases. Steadiness of both  $H_c$  and  $\chi$  values starts after 7 pulse steps. It means that after 7 steps for these metallic glass, nucleation and then partially nanostructure started.  $H_c$  and  $\chi$  values for  $Fe_{77}Cr_2Si_5B_{16}$  can be seen from Fig. 5.

A general trend of the  $\chi$  plots are similar for all three samples as shown in Fig. 3, Fig. 4 and Fig. 5. However there are some slight differences, such as sharp increase of the  $\chi$  and sharp decrease of the  $H_c$  were observed. First  $H_c$  value was high and after some pulse steps,  $H_c$  values decline to a minimum. After this relief, stability occurred because of the stress relaxation. And then some gradually increasing of the curve observed because of the

nucleation and appearance of nanocrystalisation. Some differences between the  $H_c$  and  $\chi$  plots of the samples have been observed which can be explained as composition effects.

### 3.2. XRD and SEM Results

X-ray patterns showed similar change to nanostructure as in the  $H_c$  and  $\chi$  studies. By PAM treatments, we reached after 12 pulses to the nanostructure. X-ray analysis of as-cast and 12 steps annealed  $Fe_{40}Ni_{40}B_{20}$  metallic glass samples were presented in Fig. 6. There was no Bragg peaks but only amorphous halo observed for as-received sample at  $\theta=45.44^\circ$ . At the same  $\theta$  value, for the annealed sample there was a peak observed as a sign of nucleation and nanocrystallization, similar amorphous state with a nanocrystalline solid was observed [7]. Without any addition of impurities, just using the PAM, nucleation occurred and nanocrystallization observed. When we checked the SEM pictures, similar behaviors were obtained. Fig. 7 shows the SEM analysis of the amorphous phase of as-received  $Fe_{40}Ni_{40}B_{20}$  and nanostructure phase of the sample. Fig. 7(a) represents the SEM analysis of the as-received sample which has no evidence of nucleation or crystallization. But it is clearly seen from Fig. 7(b) that after 12 pulses annealing some partially nanostructure appeared. Without changing with the composition of the sample, it is possible to get nanostructure property by using PAM. It can be clearly seen from SEM pictures that, the structure is nanometric scale. It is obvious that increasing the pulse numbers caused to fully crystal structure after some phase transformation of the sample. Pulse annealing method is a perfect method to control the structure of metallic glasses and similar alloys.

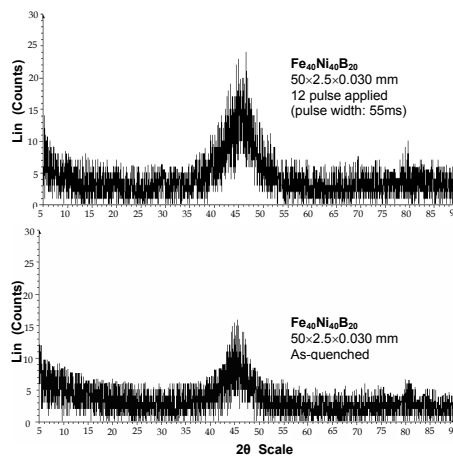


Fig. 6. X-Ray analysis of a) as-quenched and b) 12 pulse applied  $Fe_{40}Ni_{40}B_{20}$  metallic glass samples.

The FMR spectra belonging to as-quenched and annealed  $Fe_{40}Ni_{40}B_{20}$  samples at out of plane geometry were represented in Fig. 8. As it is seen from this figure, both sample exposed classical ferromagnetic behavior. The low field resonance signal was attributed to the dragging FMR mode of magnetization. The main FMR mode shows strong anisotropic behavior at out of plane geometry. At in-plane geometry, we didn't observe any anisotropic behavior for both samples.

Fig. 9. represents the angular dependence of resonance fields for out-of-plane geometry measurements at room temperature. As can be seen from Fig. 9, metallic glass exhibits very strong magnetic anisotropic behavior for out of plane. The resonance field variation increases as nanostructure state appears with annealing 12 pulses.

The value of g-factor was calculated from the variation of resonance field with rotation angle of sample at out of plane geometry as 2.19 for both samples. The calculated effective magnetic anisotropy for the as-quenched sample is 750 Oe and for the pulse applied sample is 820 Oe as shown in Fig. 9.

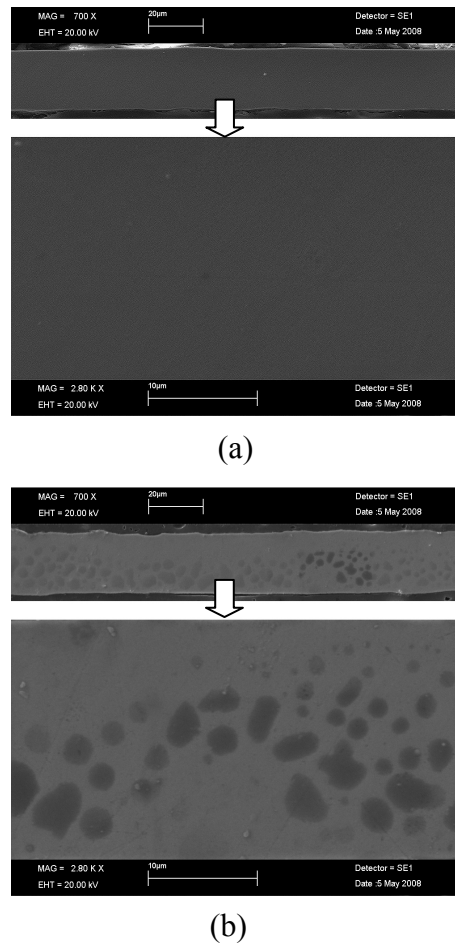


Fig. 7. SEM analysis of a) as-quenched and b) 12 pulse applied  $Fe_{40}Ni_{40}B_{20}$  metallic glass samples.

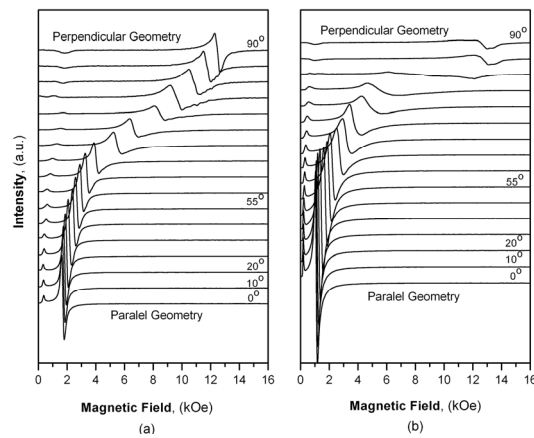


Fig. 8. The measured FMR spectra at out of plane geometry belong to the (a) as-quenched sample and (b) 12 pulse applied  $Fe_{40}Ni_{40}B_{20}$  sample.

One of the proof of the transformation from amorphous to nanocrystal also can be identified angular dependence of resonance fields at room temperature. The thickness of  $Fe_{40}Ni_{40}B_{20}$  metallic glass sample used in FMR spectra analysis was 0.030 mm. The heat treatment of metallic glasses by using pulse annealing shows the increment at effective magnetic anisotropy of the sample as increment at coercive field due to the crystallization of the sample during pulse process. The results are in agreement with previous work [12].

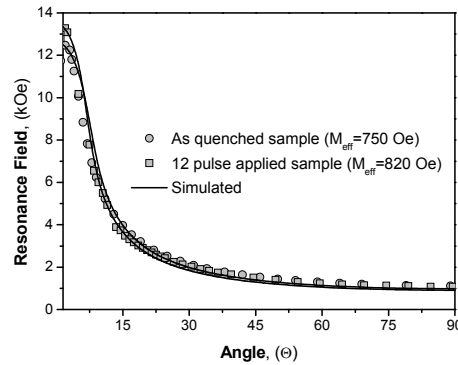


Fig. 9. The angular variation of resonance fields of as-quenched and 12 pulse applied  $Fe_{40}Ni_{40}B_{20}$  metallic glass sample.

In Fig. 9 the filled circle represent the angular variation of resonance field of as quenched sample, filled square represent the angular variation of resonance field of as pulse applied sample and solid line represent the fitted value.

#### 4. Conclusions

Nowadays, pulse annealing method is a very easy and considerable way to get nanostructure from amorphous or metallic glass materials. Annealing can be performed without oxidation and nanostructured by PAM. Controllable phase transformations also can be done. PAM is an easy and cheap way to reach better magnetic and electrical properties than conventional annealing methods. Low coercivity and high susceptibility observed with this method. Finally this method is recommended as a suitable for annealing process especially metallic glasses and amorphous ribbons.

#### 5. Acknowledgement

The authors are grateful to Professor Mike R. J. Gibbs from the University of Sheffield Engineering Material Department for his supports and valuable suggestions.

#### 6. References

- [1] T. Jagilinski, IEEE Trans. Mag. **19** 1925 (1983).
- [2] Y. Yoshisawa, S. Oguma and K. Yamauchi, J. Appl. Phys. **64** 6044 (1988).
- [3] P. D. Hudson, PhD Thesis, University of Cambridge, UK. (1986).
- [4] J. Gonzales, M. Vaszguez, J. M. Barandiran, V. Madurgan and A. Hernanda, J. Magn. Mat. **36** 73 (1983).
- [5] M. R. J. Gibbs, IEEE Transactions on Magnetics, **20** (5) 1373 (1984).
- [6] M. L. Trudeau, Nanostructured Materials, **12** (1-4) 55 (1999).
- [7] A. D. Crisian, O. Crisian, I. Skorvanek and N. Randrianantoandro, Journal of Optoelectronics and advanced Materials, **10** (4) 786 (2008).

- [8] R. Şahingöz, M. R. J. Gibbs, K. Çolakoğlu, Turkish Journal of Physics **20** 1287 (1996).
- [9] H. Fukunaga, K. Tokunaga and J. M. Song, IEEE Trans. Magn. **38** 2970 (2002).
- [10] P. Squire, S. M. Sheard, C. H. Carter and M. R. J. Gibbs J. Phys. E; Sci. Instrum. **21** 1167 (1998).
- [11] R. Şahingöz, M. Erol and M. R. J. Gibbs, J. Magn. Magn. Mater. **271 (1)** 74 (2004).
- [12] Z. Frait, D. Fraitová, N. Zakubova, P. Duhaj, Physica Status Solidi (a) **101 (1)** 239 (1987).